RSC Advances

RSC Advances

www.rsc.org/advances

ROYAL SOCIETY OF CHEMISTRY

www.rsc.org/advances

Preparation of surface self-concentration and contact-killing antibacterial coating through UV curing

Ren Liu, Junchao Zheng, Zhiquan Li, Jingcheng Liu and Xiaoya Liu*

The Key Laboratory of Food Colloids and Biotechnology, Ministry of Education, School of

Chemical and Material Engineering, Jiangnan University, Wuxi 214122, China

A facile method to prepare surface self-concentration antibacterial coating with

contact-killing mechanism was developed. Photo curable quaternary ammonium compound

QAC bearing a 16-carbon alkyl chain and a terminal methacrylate was synthesized as

reactive antibacterial additive. After UV irradiation, QAC was crosslinked in the soy-based

coating matrix. With proper amounts of QAC, the UV cured coatings exhibited good

properties such as high glossiness, good hardness and fine adhesion to cherrywood substrates.

The self-concentration property of QAC on the cured coating surface, which is beneficial to

reserve the physical properties of the bulk materials and to improve the surface antibacterial

activity, was confirmed by fluorescence and X-ray photoelectron spectroscopy. Moreover, the

introduction of QAC provided the coatings with superhydrophilicity property as well as good

anti-fog capacity. The coatings with 8 wt% of QAC (charge density = 8.6 mol/cm^2) exhibited

almost 100% antibacterial activity against Gram-positive *Staphylococcus aureus* and

Gram-negative *Escherichia coli* by 5 log reduction. The contact-killing mechanism of

coatings was confirmed via the zone of inhibition tests. The straightforward preparation

1

combined with excellent antibacterial property makes the QAC containing coatings quite promising in antibacterial coatings realm and is suitable for industrial-scale manufacturing.

Introduction

The growth and accumulation of microorganisms on surfaces are of great concern in many realms such as medical devices, healthcare products or equipments, household sanitation[1,2]. A conventional way of imparting the surfaces with antimicrobial properties is by coating with antimicrobial agents such as antibiotics [3-6], silver [7-9], copper [10-12], and peptides [13,14]. The antibacterial mechanism is based on the releasing principle of gradually leaching biocides in the surroundings. The main drawback of this type of antibacterial mechanism is the loss of antibacterial ingredients, inactivating the surface, and releasing the undesirable toxic biocides in the environment.

Alternatively, many researches have been conducted to impart the surfaces with antimicrobial properties by chemically tethering bactericidal functionalities or biocides to surfaces using various modification techniques [15-17]. The antimicrobial effect is achieved by the contact killing, without releasing the biocides in the environment. Therefore, modifying the antimicrobial surface by immobilizing nontoxic biocides or functionalities is regarded as one of the most promising approaches[1,2,18]. However, some of the surface derivatization methods are involving several synthetic steps, as well as harsh reagents and complicated process[19-21], which lack maneuverability and are probably not practical for end-use

2

application. Therefore, to develop more facile modification method without complex and expensive manufacturing steps is essential, especially for practical applications.

Among the reported straightforward modification methods, such as sol-gel process[17] and painting-like coating technology[16], UV-curing is quite promising due to its unique economic and ecologic advantages such as high curing rate, free of solvent, broad formulation range, low energy consumption, and low space and capital requirements for curing equipment. UV cured coatings containing nanoparticles or nanocomposites as antibacterial agents have been reported[22-24]. The rapidly formed coatings after irradiation exhibit good mechanical properties as well as excellent antibacterial activity. However, most of these coatings exerted the antibacterial activity via releasing the antiseptic with the above-mentioned disadvantages. A few UV-curable coatings with contact-killing antibacterial mechanism were also prepared. Chen[15] synthesized two kinds of cationic UV-curable polysiloxanes functionalized with antibacterial triclosan using hydrosilylation. The functionalized polysiloxanes were used to produce UV-curable coatings with contact-killing antibacterial activity and reasonably good mechanical properties. Our group synthesized a series of bio-based antibacterial methacrylates derived from tannic acid and successfully applied them in the non-releasing UV-curable antibacterial coatings[25].

In this paper, a quaternary ammonium compound QAC with a long aliphatic chain and a terminal methacrylate, as both the antibacterial additive and photo curable monomer, was synthesized in one step. The UV curing process was characterized by real-time infrared spectroscopy. The effect of the content of QAC on curing kinetics and basic coating

properties was systematically investigated. The surface properties of the coatings like wettability and self-concentration were also studied. The zone of inhibition tests and bacterial log reduction tests were conducted to confirm the antibacterial mechanism and evaluate the antibacterial activity of the coatings. With a proper amount of QAC, the coating exhibited excellent antibacterial activity as well as good mechanical properties, which shows promise in antibacterial coatings realm.

Experimental section

Materials

The main chemicals used are listed in Table 1. All the chemicals were used as received.

Table 1

Synthesis of photo curable quaternary ammonium compound QAC

QAC was prepared by the following procedure[26]. DMAEMA (2.36 g, 0.015 mol) and methoxyphenol (0.03 g, 0.1 wt%) were mixed in 30 mL acetonitrile in a 100-mL round-bottom flask equipped with a reflux condenser, followed by adding HB (5.18 g, 0.017 mol). Then, the mixture was stirred and refluxed for 24 h. The resulting reaction mixture was precipitated in anhydrous diethyl ether, and white solid precipitate was filtered from the solution by suction filtration, recrystallized in absolute ethanol, and finally dried in a vacuum oven for 24 h to afford product QAC (6.53 g) in 86.7% yield.

^{1}H-NMR (400 MHz, CDCl$_3$) : δ 6.15 (s, 1H), 5.67 (s, 1H), 4.67 (dd, *J* = 5.6, 3.4 Hz, 2H), 4.25 – 4.12 (m, 2H), 3.72 – 3.59 (m, 2H), 3.56 – 3.47 (m, 6H), 1.95 (s, 3H), 1.78 (d, *J* = 7.6 Hz, 2H), 1.47 – 1.10 (m, 26H), 0.88 (t, *J* = 6.8 Hz, 3H).

Attenuated total reflectance Fourier transform infrared (ATR-FTIR): 2845–2920 cm^{-1} (saturated C–H stretching vibration), 1720.5 cm^{-1} (C=O stretching vibration), 1634.8 cm^{-1} (C=C stretching vibration), 720.9 cm^{-1} (CH$_2$)$_n$ > 4 rocking vibration.

Coating formulation and antibacterial coating preparation

The soy-based UV-curable coatings were formulated as listed in Table 2. Gentle heating was used for the dissolution of the photoinitiator when necessary. The liquid coatings were casted on cherrywood for basic properties tests with a drawdown block(60 μm) to form a thin film followed by UV curing using a Fusion LC6B benchtop conveyor with an F300 UVA lamp (UVA intensity of 120 mW/cm^2 measured using a UV-int140 from DESIGN Germany) in the air. The general curing protocol was three passes through the lamp at a conveyer belt speed of 5 m/min. The coatings were tested after being conditioned in ambient conditions for at least 48 h.

Table 2

Analysis of UV-curing process of coatings

Real-time infrared (RTIR) spectroscopy was used to analyze the UV-curing process of photosensitive formulations under UV irradiation. The coating formulations were coated on a KBr window and then irradiated with an EfosLite mercury vapor curing lamp equipped with a fiber optic light guide for 600 s at an intensity of 40 mW/cm^2. All the experiments were

performed in air. The change in the peak area of the double bond peak at 810 cm^{-1} was recorded at a resolution of 8 cm^{-1}. For each sample, a series of RTIR runs were repeated thrice. The degree of conversion was calculated from Eq. (1)

$$\text{Degree of Conversion} = \left\{ \frac{[(A)_{810}]_0 - [(A)_{810}]_t}{[(A)_{810}]_0} \right\} \times 100 \quad (1)$$

where $[(A)_{810}]_0$ is the absorption peak area before UV exposure, whereas $[(A)_{810}]_t$ is the absorption peak area after UV exposure.

Characterization of basic properties of coatings

Gloss measurements were performed using a BYK Gardner micro-TRI-gloss meter, and the mean of these measurements was recorded. Pencil hardness and pendulum hardness were measured following ASTM D3363 and ASTM D4366 protocols, respectively. Crosshatch adhesion was measured according to ASTM D3359 protocol. The gel content was determined by measuring the weight loss after 24 h of extraction with acetone, according to ASTM D2765-84 protocol.

Thermogravimetric analysis (TGA) of the prepared coatings (~10 mg) was performed using a Mettler Toledo STAR thermogravimetric analyzer at a heating rate of 15 °C/min from 25 to 600 °C. Nitrogen was used as the purge gas at a flow rate of 50 mL/min. The temperature at 10% weight loss(T_d10) was used to access the thermal stability of coatings.

Characterization of surface properties of coatings

The water and oil wettability of the UV-cured coatings were determined by the contact angles of water and oil drops at the surface. 1-Bromonaphthalene was used as an oleophilic organic compound. γ^d and γ^p for water are 21.8, 51.0 mN/m, respectively. γ^d and γ^p for 1-bromonaphthalene at 25 °C are 44.4 and 0.0 mN/m, respectively. The surface tension (γ_s) of the UV-cured coating was calculated from Eqs. (2) and (3)

$$\gamma_s = \gamma_s^d + \gamma_s^p \qquad (2)$$

$$(1+\cos\theta)\gamma_l = 4\left(\frac{\gamma_l^p \gamma_s^p}{\gamma_l^p + \gamma_s^p} + \frac{\gamma_l^d \gamma_s^d}{\gamma_l^d + \gamma_s^d}\right) \qquad (3)$$

The anti-fog capacity was evaluated by the visual inspection of the surface images, which were recorded by holding the samples above hot water (80 °C) for 15 s.

Surface charge density of the coatings was quantified using fluorescein dye [27,28]. A glass slide coated with the prepared coatings was immersed in a fluorescein sodium salt solution (10 mg/mL in deionized water) for 10 min in the dark. After rinsing extensively with deionized water, the glass slide was placed in 25 mL cetyltrimethylammonium chloride (CTAC) solution (0.1 wt% in deionized water) and shaken for 10 min to absorb the dye. Then, 10% (by volume) of an aqueous phosphate buffer (100 mM, 0.94 mg/mL monosodium phosphate monohydrate and disodium phosphate anhydrous (13.2 mg/mL) in deionized water, pH 8.0) were added to the CTAC solution. The absorbance of the resulting CTAC solution was measured at 501 nm, and the concentration of the fluorescein dye was calculated using the Beers Law with the extinction coefficient of fluorescein in this solution at 77 mM^{-1} cm^{-1}.

Study of the distribution of QAC in coating network

Fluorescence microscopic analysis was used to visualize the distribution of QAC in the UV-cured coating network. The coating was cut into pieces and treated with an aqueous solution of 0.03 M fluorescein sodium, which is known to selectively bind to quaternary ammonium groups for 24 h[29]. Then, the coating pieces were washed with water for 2 days, and images of the cross-sections of the coating pieces were recorded using a fluorescence microscope.

X-ray photoelectron spectroscopy analysis (XPS) was used to determined the concentration of QAC on the surface or bottom of the coating samples. The spectra were recorded with Al Kα line as the excitation source (hv = 1486.6 eV). The binding energy (BE) values were referenced to the C 1s peak of the contaminant carbon at 284.8 eV.

Antimicrobial test procedure

Cultures of *Staphylococcus aureus* and *Escherichia coli* were grown aerobically for 10 h at 37 °C in sterile Luria–Bertani (LB) broth (normal rich growth medium: NaCl, 10 g/L; yeast extract, 5 g/L; trypton 10 g/L). The bacterial solutions were diluted in saline (8.5 g/L), and the concentrations were evaluated quantitatively by measuring OD_{600nm}.

(1) Zone of inhibition test. The films containing 10 wt% QAC were prepared to test for any possible leaching of the active QAC species. The plates were inoculated at a level of 10^6 cfu/ml *Escherichia coli* bacteria. The films (1.5×1.5 mm^2) were placed on agar plates with their active side on the agar. After 24 h incubation in 37 °C incubator, the zone of inhibition

around the films was evaluated. Any possible leaching of the active QAC species would inhibit the bacterial growth around the films.

(2) Antimicrobial activity determination of prepared coatings. The bacterial log reduction test was followed according to the reported procedure[30] and is similar to the standard antimicrobial susceptibility test protocols such as ISO 22196 and JIS Z 2801. The obtained bacterial solutions were distributed over 12-well cell plates containing 1.5×1.5 mm^2 coating, except for the control well without coating. After incubation at 37 °C for 24 h, each treatment was serially diluted and 100 μL of three dilutions were plated on a sterile LB agar plate (LB broth + agar 20 g/L). After 24 h, the number of colonies on each plate was determined to get the corresponding concentration of living bacteria.

The aerosol method[25,31] for determining surface antimicrobial activity was done to visually exhibit the antibacterial ability of coatings. Aqueous suspension of *E.coli* and *S. aureus* (10^4-10^5 CFU/mL) was casted onto the prepared slides by aerosol spraying. After air-drying for 5 min, the glass slides were cultivated overnight at 37 ℃ under autoclaved growth agar. Then, the grown bacterial colonies were inspected and counted to evaluate the antibacterial performances.

Results and discussion

(1) Photopolymerization of the formulations containing different amount of QAC

To evaluate the influence of antibacterial QAC to the crosslinking degree and polymerization rate of coatings, the polymerization kinetics of formulations with different amount of QAC

were monitored by real-time FTIR. The conversion and curing rate (R_p) as a function of time curve are shown in Fig.1. The final double bond conversion is effected by the addition of QAC, varies from 70% for QAC-0% to 65% for QAC-8%, while 52% for QAC-15%. It is because the QAC was monofunctional quaternary ammonium compound which acts as a chain extender, and its addition to UV-curing system may do negative effect to polymerization kinetics of coatings. The same trend was also observed for the relationship between the curing speed and QAC content. The maximum rate ranges from 6.8 s^{-1} for QAC-0% to 5.4 s^{-1} for QAC-8%, while 2.7 s^{-1} for QAC-15%. Therefore, too high level of QAC content was not desired and no more than 8% QAC content is proper for the soy-based UV-curable system.

Fig.1

(2) Basic properties of UV-Cured Coatings

The basic properties of the UV-cured coatings are studied and listed in Table 3. The 60 degree gloss value was very high from 171 to 173. The pencil hardness and pendulum hardness are H~2H, 35~45s, respectively. Since the ultimate hardness value is closely related to crosslinking degree of coating network. The hardness decreased slightly with increased QAC addition which is attributed to decreasing crosslinking degree shown in the real-time FTIR results (Fig. 1). From the gel content and T_d10 results, the same trend was observed. All the gel contents were very high(≥90%), although the introduction of QAC led a decrease of the gel content. T_d10 varied from 335.6 ℃ for QAC-0% to 285.5 ℃ for QAC-15% coating, indicating the QAC addition reduce the thermal stability of coatings to some extent. All the

coatings show good adhesion to cherrywood substrate, despite the content of monofunctional

QAC in the formulations.

Table 3

(3) Surface properties of UV-Cured Coatings

The synthesized monofunctional QAC had good solubility in water. The effect of its

hydrophilicity on the coating surface wettability, surface energy and bulk properties were

evaluated by water/oil contact angle measurements and water immersion test(supporting

information), respectively. Fig. 2(A) shows the water/oil contact angles and surface energy of

the UV-cured coatings with different concentrations of QAC. The addition of QAC

significantly increased the coating hydrophilicity with a sharp decrease in water contact angle

from 70 to <10°. For the oil test, the changes in contact angle were not significant. The γ_s of

the UV-cured films were calculated, indicating an evident increase from 54.9 to 79.4 mJ m^{-2}

with the incorporation of the QAC. It is reported that surface wettability is a decisive

parameter determining the magnitude of initial microbial adhesion. Hydrophilic surfaces are

usually more resistant to microbial adhesion than hydrophobic ones[32-34]. Fig. 2(B) shows the

anti-fog images of QAC-10% and QAC-0% (control) coatings, indicating that QAC-10%

sample exhibits good transparency, demonstrating its good anti-fog capacity. The anti-fog

capacity of antibacterial coatings may extend their applications in some unique realms where

anti-fog ability and sterility is needed.

Fig. 2

(3) Distribution of the QAC in the network

11

The fluorescence microscopic images are shown in Fig. 3. Fig. 3(A) shows the image of

coating network containing no QAC, whereas 10 wt% QAC was included in the coating

network in Fig. 3(B). A bright fluorescent section, evoked by the fluorescence dye, was

observed on the liquid–air interface of the coating network in Fig. 3(B). Comparing to the

observation in Fig. 3(A) with no fluorescence in the interface, it is concluded that the

self-concentration of QAC at the surface occurred. The result can be also supported by the

XPS analysis, shown in Fig. 4. The %N on the surface is much higher than that at the bottom

of QAC-10% coating. The enrichment at the surface may be a consequence of poor

compatibility between amphiphilic salts and soy-based resins. The self-concentration of

antimicrobial agents at the surface is advantageous not only to preserve the physical

properties of the bulk materials, but also to offer more effective antibacterial activity than

antimicrobial agents that are distributed through the coating[35].

Fig. 3

Fig. 4

(4) Antimicrobial activity determination of coatings

The antimicrobial activity of the prepared coatings was investigated for Gram-positive

S.aureus and Gram-negative *E. coli* by monitoring the decrease in the number of colony

forming units (cfu) in 24 h. In this study, 10^5 CFU/mL is used as the starting bacterial

concentration, described in the ISO 22196 protocol.

In the soy-based UV-curable coatings, QACs are the effective antibacterial agents which impart the coatings antibacterial ability. To make sure that it's the QACs chemically tethered in coating matrix, that exhibit antibacterial activity and no free QACs was released, the zone of inhibition test was carried out. The results of zone of inhibition test was shown in Fig. 5. QAC-10% films did not show any inhibition zone, thus no leaching of QACs occurred from QAC-10% films, indicating that the antibacterial effect of the system is based on the contact-killing mechanism.

For contact-killing mechanism, the charge density brought by tethered QACs play an important role in antibacterial activity. The surface charge density was calculated using a ratio of 1:1 for fluorescein dye molecules to quaternary ammonium groups, and the results are shown in Fig. 6. With increasing QAC content, the charge density of the coating surfaces showed an evident increase from $(2.51 \pm 0.21) \times 10^9$ mol·cm^{-2} for QAC-1% to $(17.5 \pm 0.26) \times 10^9$ mol·cm^{-2} for QAC-15%. And the antibacterial activity of coatings improves accordingly. When the QAC content was $\geq$ 8 wt%(charge density $\geq$8.6 mol/cm^2), the corresponding coating showed the maximum antibacterial effect against *E. coli* and *S. aureus* (5 log reduction, almost 100% killing efficiency). The antibacterial activity leveled off for the further increased amount of QAC

Fig. 7 displayed the antimicrobial results of QAC-0% and QAC-10% coated glass slide against Gram-positive Staphylococcus aureus and Gram-negative Escherichia coli. Numerous colonies of bacteria grew on QAC-0% coating slides while   much less bacteria were

observed on the slides coated with QAC-10%. The results indicated that QAC-10% coating

slides exhibited stronger antimicrobial property than QAC-0%.

Fig. 5

Fig. 6

Fig.7

Conclusions

In summary, a facile method to prepare self-concentration antibacterial coating with

contact-killing mechanism was developed. A quaternary ammonium compound QAC with a

long aliphatic chain and a terminal methacrylate, as both the antibacterial agent and photo

curable monomer, was synthesized in one step. The increased amount of QAC (up to 15 wt%)

decreased the final double bond conversion and curing speed and no more than 8 wt% of QAC

was found to be proper in the soy-based UV-curable formulation. Although the introduction

of QAC weaken some of the basic properties of coatings, all the coatings were still shown

reasonably good properties with high glossiness, good hardness and fine adhesion to

cherrywood substrate. The introduction of QAC provided the coatings with

superhydrophilicity property as well as good anti-fog capacity, which would extend the

application range of the coatings. The results of fluorescence and XPS confirmed the

self-concentration property of QAC on the cured coating surface, which is beneficial to reserve

the physical properties of the bulk materials and to improve the surface antibacterial activity.

When the QAC content was $\geq 8\%$ (charge density ≥ 8.6 mol/cm^2), the coatings exhibited almost

14

100% antibacterial activity against Gram-positive *Staphylococcus aureus* and Gram-negative *Escherichia coli* by 5 log reduction. The zone of inhibition tests confirmed the contact-killing mechanism and no free QAC was leased. The straightforward preparation combined with excellent antibacterial property makes the QAC containing coatings quite promising in antibacterial coatings realm.

Acknowledgements

References

1 J.C. Tiller, *Adv. Polym. Sci.*, 2011, **240**, 193–217.

2 E. R. Kenawy, S. D. Worley, R. Broughton, *Biomacromolecules*, 2007, **8**, 1359–1384.

3 D. Chung, S. E. Papadakis, K. L. Yam, *Int. J. Food. Sci. Technol.*, 2003, **38**, 165–169.

4 T. Jin, H. Zhang, *J. Food. Sci.*, 2008, **73**, 127–134.

5 A. Guarda, J. F. Rubilar, J. Miltz, M. J. Galotto, *Int. J. Food. Microbiol.*, 2011, **146**, 144–150.

6 A. Piozzi, I. Francolini, L. Occhiaperti, M. Venditti, W. Marconi, *Int. J. Pharm.*, 2004, **280**, 173–183.

7 E. Abdullayev, K. Sakakibara, K. Okamoto, W. Wei, K. Ariga, Y. Lvov, *ACS Appl. Mater. Inter.*, 2011, **3**, 4040–4046.

8 P. DeVasConCellos, S. Bose, H. Beyenal, A. Bandyopadhyay, L. G. Zirkle, *Mater. Sci. Eng. C.*, 2012, **32**, 1112–1120.

15

9 J. Song, H. Kang, C. Lee, S. H. Hwang, J. Jang, *ACS Appl. Mater. Inter.*, 2011, **4**, 460–465.

10 B. Jia, Y. Mei, L. Cheng, J. Zhou, L. Zhang, *ACS Appl. Mater. Inter.*, 2012, **4**, 2897–2902.

11 O. Sharifahmadian, H. R. Salimijazi, M. H. Fathi, J. Mostaghimi, L. Pershin, *Surf. Coat. Tech.*, 2013, **233**, 74–79.

12 M. D. Teli, J. Sheikh, *Int. J. Biol. Macromol.*, 2013, **61**, 302–307.

13 M. Zasloff, *Nature*, 2002, **415**, 389–395.

14 Y. Li, K. N. Kumar, J. M. Dabkowski, M. Corrigan, R. W. Scott, K. Nüsslein, G. N. Tew, *Langmuir*, 2012, **28**, 12134–12139.

15 Z. Chen, B. Chisholm, S. Stafslien, J. He, S. Patel, *J. Biomed. Mater. Res. part A*, 2010 **95**, 486–494.

16 D. Park, J. Wang, A. M. Klibanov, *Biotechnol. Progr.*, 2006, **22**, 584–589.

17 M. J. Saif, J. Anwar, M. A. Munawar, *Langmuir*, 2008, **25**, 377–379.

18 J.A. Lichter, K. J. V. Vliet, M. F. Rubner, *Macromolecules*, 2009, **42**, 8573–8586.

19 S. B. Lee, R. R. Koepsel, S. W. Morley, K. Matyjaszewski, Y. Sun, A. J. Russell, *Biomacromolecules,* 2004, **5**, 877–882.

20 S. Y. Wong, J. S. Moskowitz, J. Veselinovic, R. A. Rosario, K. Timachova, M. R. Blaisse, R. C. Fuller, A.M. Klibanov, P. T. Hammond, *J. Am. Chem. Soc.*, 2010, **132**, 17840–17848.

21 R. Müller, A. Eidt, K. A. Hiller, V. Katzur, M. Subat, H. Schweikl, S.Imazato, S. Ruhl, G. Schmalz, *Biomaterials*, 2009, **30**, 4921–4929.

22 A. L. Motlagha, S. Bastani, M.M. Hashemi, *Prog. Org. Coat.*, 2014, **77**, 502–511.

23 I. Larraza, C. Peinado, C. Abrusci, F. Catalina, T. Corrales., *J. Photoch. Photobio. A*, 2011, **224**, 46–54.

24 G. Gozzelino, G. A. Dell Aquila, D. Romero Tobar. *J. Appl. Polym. Sci.*, 2009, **112**, 2334–2342.

25 R. Liu, J. Zheng, R. Guo, J. Luo, Y. Yuan, X. Liu, *Ind. Eng. Chem. Res.* 2014, **53**, 10835–10840.

16

26 G. Lu, D. Wu, R. Fu, *React Funct. Polym.*, 2007, **67**, 355–366.

27 J. C. Tiller, C. J. Liao, K. Lewis, A. M. Klibanov, *Proc. Natl. Acad. Sci.*, 2001, **98**, 5981–5985.

28 J. M. Antonucci, D. N. Zeiger, K. Tang, S. Lin-Gibson, B. O. Fowler, N. J Lin, *Dent. Mater.*, 2012, **28**, 219–228.

29 J. W. Ledbetter Jr, J. R. Bowen, *Anal. Chem.*, 1969, **41**, 1345–1347.

30 J. H. Wynne, P. A. Fulmer, D. M. McCluskey, N. M. Mackey, J. P. Buchanan, *ACS Appl. Mater. Inter,* 2011, **3**, 2005–2011.

31 J. Lin, S. Qiu, K. Lewis, A. M. Klibanov, *Biotechnol. Progr.*, 2002, **18**, 1082–1086.

32 Y. H. An, R.J. Friedman, *J. Biomed. Mater. Res.*, 1998, **43**, 338–48.

33 M. Katsikogianni, Y. F. Missirlis, *Eur. Cell. Mater.*, 2004, **8**, 37–57.

34 J. Chandra, J.D. Patel, J. Li, G. Zhou, P. K. Mukherjee, T. S. McCormick, J. M. Anderson, M. A. Ghannoum. *Appl. Environ. Microbiol.*, 2005, **71**, 8795–801.

35 M. B. Harney, R. R. Pant, P. A. Fulmer, J. H. Wynne, *ACS Appl. Mater. Inter.*, 2008, **1**, 39–41.
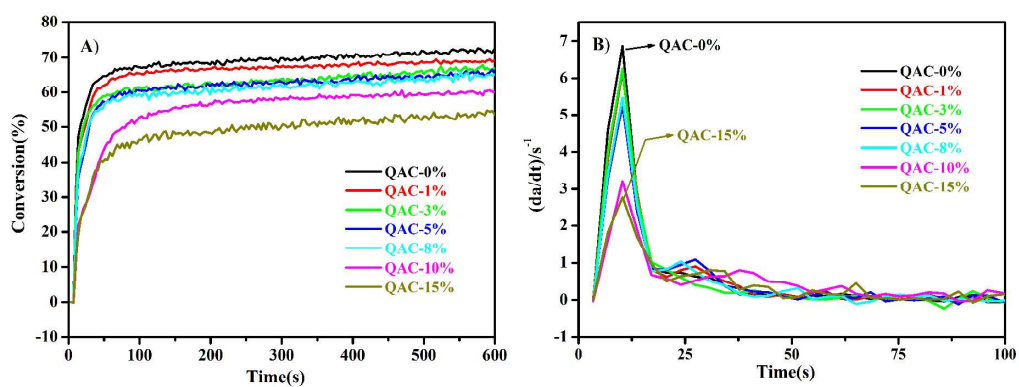
Fig.1 Photopolymerization rate comparison of the formulations containing QAC from 0 to 15

wt%. A), B) : double bond conversion and R_p on irradiation time, respectively.
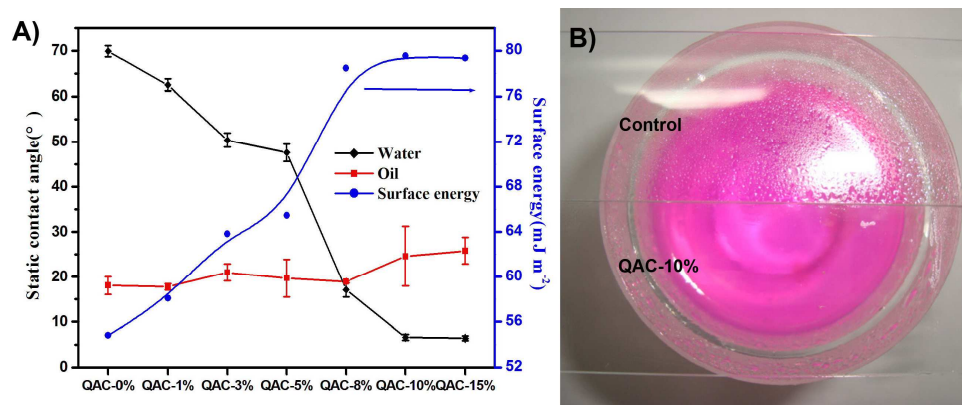
Fig. 2 (A) Static contact angle and surface energy of coatings with different concentrations of

QAC; (B) Images of anti-fog test of QAC-10% and QAC-0% (control) coatings on glass
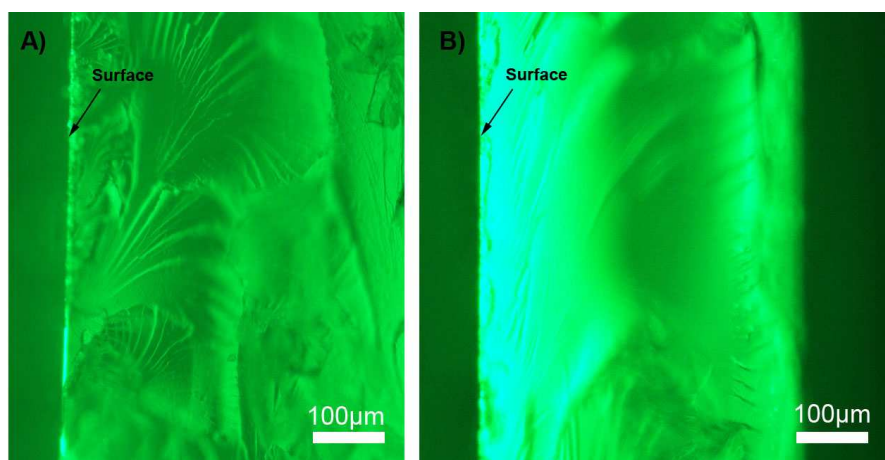
slides.

Fig. 3 Fluorescence images of the UV-cured coatings: A) QAC-0% and B) QAC-10% stained
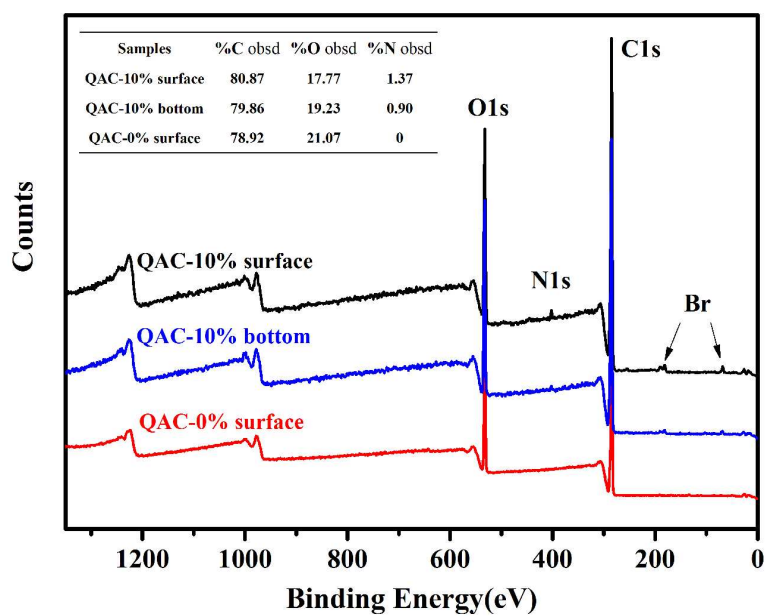
with fluorescence dye.

Fig. 4 XPS survey spectra at the surface, bottom of QAC-10% coating and the surface of
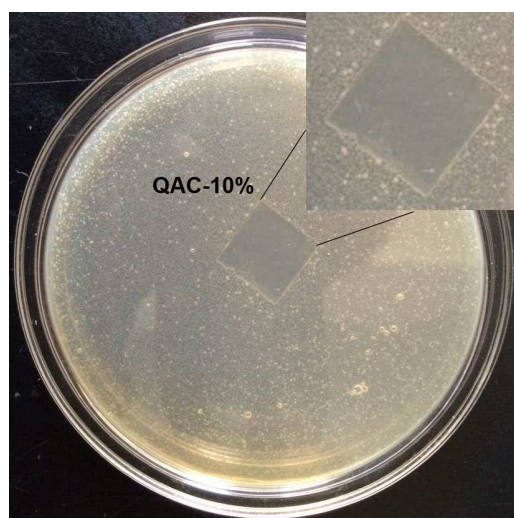
QAC-0% coating.

Fig. 5 Picture of a zone of inhibition test results of QAC-10% coating against *E.coli.*

Fig. 6 Bacterial log10 reduction after 24 h incubation of 10^5 bacteria with 1.5×1.5 mm^2

prepared films and surface charge density of films containing different amounts of QAC.

Fig.7 Photographs of bacteria colonies grown on glass slides: A) coated with QAC-0% against

E.coli, B) coated with QAC-10 against *E.coli* ; C) coated with QAC-0% against *S.aureus*, D)

coated with QAC-10% against *S.aureus.*

Table 1 Main chemicals used.

Table 2 Recipe for UV-curable antibacterial coating formulation.

Table 3 The properties of the UV-cured coatings.

Fig.1 Photopolymerization rate comparison of the formulations containing QAC from 0 to 15 wt%.

A), B) : double bond conversion and R_p on irradiation time, respectively.

Fig. 2 (A) Static contact angle and surface energy of coatings with different concentrations of QAC; (B) Images

of anti-fog test of QAC-10% and QAC-0% (control) coatings on glass slides.

Fig. 3 Fluorescence images of the UV-cured coatings: A) QAC-0% and B) QAC-10% stained with fluorescence

dye.

Fig. 4 XPS survey spectra at the surface, bottom of QAC-10% coating and the surface of QAC-0% coating.

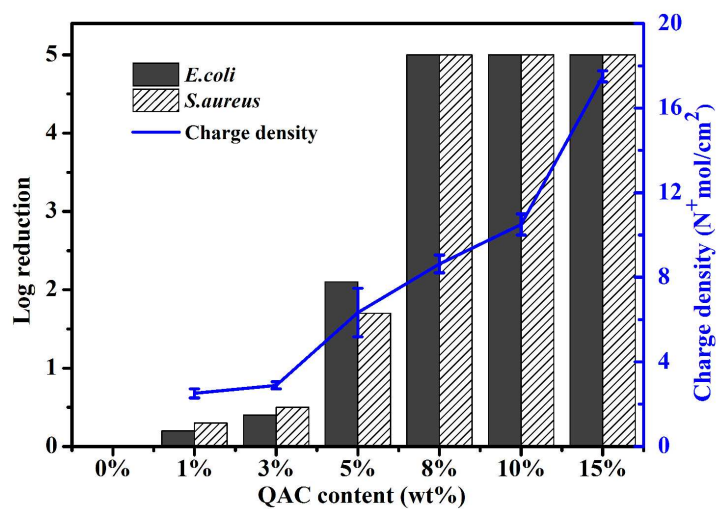Fig. 5 Picture of a zone of inhibition test results of QAC-10% coating against *E.coli*.

Fig. 6 Bacterial log10 reduction after 24 h incubation of 10^5 bacteria with 1.5×1.5 mm^2 prepared films and

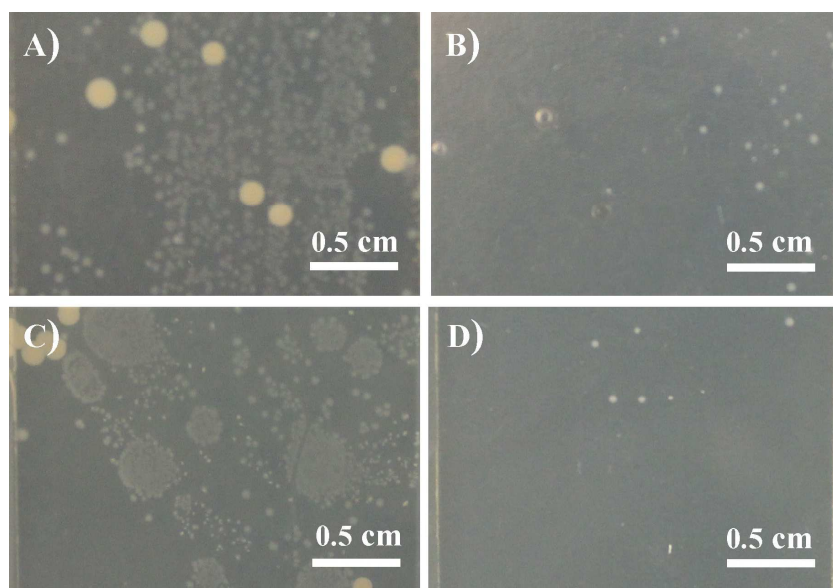surface charge density of films containing different amounts of QAC.

Fig.7 Photographs of bacteria colonies grown on glass slides: A) coated with QAC-0% against *E.coli*, B) coated

with QAC-10 against *E.coli* ; C) coated with QAC-0% against *S.aureus*, D) coated with QAC-10% against

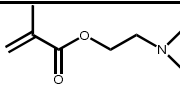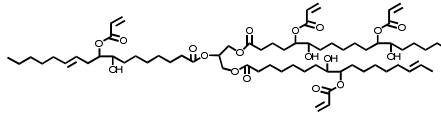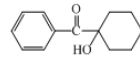*S.aureus.*

Table 1 Main chemicals used.

Name	Abbreviation	Source	Generic structure and description
Dimethylaminoethyl methacrylate	DMAEMA	Aladdin	
1-Bromohexadecane	HB	Shanghai Chemical Reagent Co., Ltd	
SM6103	AESO	Jiangsu Sanmu group company	
CN2302	HBP	Sartomer	Hyperbranched polyester acrylate
CD9051	AP	Sartomer	Phosphated acidic adhesion promoter
Irgacure184	PI	BASF chemicals	

Table 2 Recipe for UV-curable antibacterial coating formulation.

Sample	AESO (wt%)	HBP (wt%)	QAC (wt%)	PI (wt%)
QAC-0%	67	30	0	3
QAC-1%	66	30	1	3
QAC-3%	64	30	3	3
QAC-5%	62	30	5	3
QAC-8%	59	30	8	3
QAC-10%	57	30	10	3
QAC-15%	52	30	15	3

Table 3 The properties of the UV-cured coatings.

Properties	QAC-0%	QAC-1%	QAC-3%	QAC-5%	QAC-8%	QAC-10%	QAC-15%
Gloss (60°)	173±0.9	171±0.3	172±0.4	171±0.8	172±0.9	172±1.5	172±1.4
Pencil hardness	2H	2H	2H	H	H	H	H
Pendulum hardness	45±1	43±0	43±1	41±0	39±1	37±2	35±3
Gel content (%)	95.05±0.70	94.33±1.07	94.02±0.79	92.73±0.25	92.29±0.36	92.18±0.25	90.19±0.53
Cross-hatch adhesion	1	1	1	1	1	1	1
T_d10 (℃)	335.6	330.3	319.5	306.2	294.9	289.5	285.5

28

The straightforward preparation of surface self-concentration and contact-killing antibacterial coating through UV curing.